HHS Public Access

Author manuscript

Clin Cancer Res. Author manuscript; available in PMC 2018 November 15.

Published in final edited form as:

Clin Cancer Res. 2017 November 15; 23(22): 6993–7005. doi:10.1158/1078-0432.CCR-17-1098.

Synergy of WEE1 and mTOR inhibition in mutant KRAS-driven lung cancers

Josephine Hai[1,2], **Shengwu Liu**[1,2], **Lauren Bufe**[1], **Khanh Do**[1,2], **Ting Chen**[1,3], **Xiaoen Wang**[1], **Christine Ng**[4], **Shuai Li**[1,2], **Ming-Sound Tsao**[4], **Geoffrey I. Shapiro**[1,2], and **Kwok-Kin Wong**[1,2,3]

[1]Department of Medical Oncology, Dana-Farber Cancer Institute, Boston, MA, USA

[2]Department of Medicine, Harvard Medical School, Boston, MA, USA

[3]Perlmutter Cancer Center, New York University Langone Medical Center, New York, New York 10016, USA

[4]Princess Margaret Cancer Centre/University Health Network, Toronto, ON, CA

Abstract

Purpose—*KRAS*-activating mutations are the most common oncogenic driver in non-small cell lung cancer (NSCLC), but efforts to directly target mutant KRAS have proved a formidable challenge. Therefore, multi-targeted therapy may offer a plausible strategy to effectively treat KRAS-driven NSCLCs. Here, we evaluate the efficacy and mechanistic rationale for combining mTOR and WEE1 inhibition as a potential therapy for lung cancers harboring *KRAS* mutations.

Experimental Design—We investigated the synergistic effect of combining mTOR and WEE1 inhibitors on cell viability, apoptosis, and DNA damage repair response using a panel of human *KRAS*-mutant and wild type NSCLC cell lines and patient-derived xenograft cell lines. Murine autochthonous and human transplant models were used to test the therapeutic efficacy and pharmacodynamic effects of dual treatment.

Results—We demonstrate that combined inhibition of mTOR and WEE1 induced potent synergistic cytotoxic effects selectively in *KRAS*-mutant NSCLC cell lines, delayed human tumor xenograft growth and caused tumor regression in a murine lung adenocarcinoma model. Mechanistically, we show that inhibition of mTOR potentiates WEE1 inhibition by abrogating compensatory activation of DNA repair, exacerbating DNA damage in *KRAS*-mutant NSCLC, and that this effect is due in part to reduction in cyclin D1.

Corresponding author: Kwok-Kin Wong, MD, PhD, Laura & Isaac Perlmutter Cancer Center, NYU Langone Medical Center, 550 1st Ave., Smilow 1011, New York, NY, 10016, USA, Phone: 212-263-9203, kowk-kin.wong@nyumc.org.

Authors' contributions:

JH, KKW, KD and GS designed and conceived this study. JH, LB, SL, SL, CN, and TC performed and analyzed the results. All authors were involved in the writing and review of the manuscript.

Ethics approval:

All animal experiments were performed in accordance with procedures approved by the DFCI Animal Care and Use Committee.

Conclusions—These findings demonstrate that compromised DNA repair underlies the observed potent synergy of WEE1 and mTOR inhibition and support clinical evaluation of this dual therapy for patients with *KRAS*-mutant lung cancers.

Keywords

KRAS; WEE1; mTOR; lung adenocarcinoma

Introduction

Lung cancer is the leading cause of cancer deaths worldwide and non-small cell lung cancer (NSCLC) accounts for more than 80% of those cases (1, 2). Kirsten *RAS* viral oncogene homolog (*KRAS*) is mutated in 25–30% of lung adenocarcinomas (3). Unlike NSCLC patients harboring *EGFR*-activating mutations or *ALK* fusions, for which targeted inhibitors have achieved objective responses in up to 80% of cases, direct molecular inhibition of mutant *RAS* has proved difficult owing to its structure as well as picomolar affinity to GDP/GTP (3–6). Patients with tumors harboring *KRAS*-mutations are among the most difficult to treat and individual inhibitors targeting mutant *RAS* downstream signaling pathways such as PI3K/AKT/mTOR and RAF/MEK/ERK have yielded limited response rates of less than 20% in clinical trials (7). This suggests that RAS is associated with crosstalk of highly complex and redundant signaling cascades leading to bypass pathways and negative feedback loops (8). Complicating this, we previously showed that *KRAS*-mutant lung tumors bearing *TP53* or *LKB1* co-mutations differ in their response to docetaxel with or without selumetinib, suggesting that co-mutations may also impact treatment response (9, 10).

Given greater molecular diversity in *KRAS*-mutant tumors compared with other actionable oncogenic targets in lung adenocarcinoma, one approach to improving the clinical efficacy of inhibitors is to identify drug combinations that either target multiple RAS-driven pathways or circumvent resistance. Previously, Weisberg *et al.* used a chemical screen in a mutant NRAS-transformed Ba/F3 cell line to show that an inhibitor of WEE1, AZD1775, synergized with the mTOR inhibitor Torin2 in acute leukemia (11). mTOR is a critical downstream effector of RAS in lung cancer; however, clinical testing of mTOR inhibitors alone have demonstrated limited efficacy (12). Preclinical studies have shown that mTOR inhibitors suppress homologous recombination-mediated DNA repair (HDR) and synergize with poly (ADP-ribose) polymerase (PARP) inhibitors in BRCA1-proficient triple-negative breast cancers (13). AZD2014 is a novel small molecule ATP-competitive dual inhibitor of both mTORC1 and mTORC2 kinase that is well-tolerated in preclinical studies and is currently in phase II clinical trials (14, 15).

WEE1 is a protein kinase that negatively regulates the G2/M checkpoint by inhibiting cyclin-dependent kinase (CDK) 1 via tyrosine 15 phosphorylation (16). AZD1775 is a first-in-class, pyrazolo-pyrimidine derivative and potent small-molecule WEE1 kinase inhibitor (17). CDK1 is also necessary for BRCA1-mediated S phase checkpoint activation and HDR (18). Although previous studies have shown that WEE1 inhibitors such as AZD1775

augment the effects of chemotherapy by driving transformed cells to mitotic catastrophe, it is unclear how mTOR inhibition potentiates the effects of AZD1775(19).

Here, we investigated the mechanism underlying *KRAS*-mutant cell sensitivity to dual WEE1 and mTOR inhibition. We show that WEE1 inhibition in *KRAS*-mutant cells induces DNA damage accumulation, which is further compounded by simultaneous compromise of DNA repair, mediated by mTOR inhibition. Importantly, oral administration of mTOR and WEE1 inhibitors at clinically relevant doses caused significant reduction in human xenografted tumor growth as well as tumor regression in autochthonous lung adenocarcinoma murine models. Our results support further clinical investigation of combined WEE1/mTOR inhibition as a potential *KRAS*-driven NSCLC therapy.

Materials and Methods

Cell culture, CRISPR vectors and stable isogenic cell line generation

Human NSCLC cell lines (A427, NCI-H23, NCI-H1355, NCI-H441, NCI-H2009, NCI-H358, Calu1, NCI-H460, HCC827, HCC4006, NCI-H1975, NCI-H3255, and NCI-H1650) were obtained from the American Type Culture Collection (ATCC) and cultured in RPMI-1650 media supplemented with 10% Fetal Bovine Serum (Thermo Fisher, Waltham, MA) and antibiotics. Patient-derived xenograft (PDX) cell lines (PDX239, 267, 277 and 462) were previously derived using protocols approved by the University Health Network Human Research Ethics and Animal Care Committee (20). *KRAS* mutation status for PDX cell lines were detected using the Sequenom OncoCarta panel v1.0 (San Diego, CA) as previously described (20, 21). Human embryonic kidney 293T (HEK293T) cells were cultured in DMEM media supplemented with 10% FBS and antibiotics. All cells were cultivated at 37°C and 5% CO_2. Authentication of ATCC human cell lines and PDX cells were done by short tandem repeat DNA profiling analysis.

LentiCRISPRv2 vector containing *Sp*Cas9 (Addgene, #52961) was digested with BsmB1 and ligated with annealed oligos. Guide RNAs (gRNA) against human CCND1 were designed using CHOPCHOP (https://chopchop.rc.fas.harvard.edu; Supplemental Table 1). Retroviral constructs containing human full length *LKB1* (#8592) and kinase-dead *LKB1* (K78I) (#8593) were obtained from Addgene (Cambridge, MA) and sequence verified. Transient transfections and virus preparation in HEK293T cells were performed using Fugene reagents (Promega, Madison, WI) as per manufacturer's protocol. Retro- and lentivirus were prepared by transfecting two packaging plasmids into 293T cells using protocols from The RNAi Consortium (TRC; Broad Institute, Cambridge, MA)(22). Stable cell lines were isolated following viral transduction and selection with puromycin antibiotics (1–2 μg/mL).

Human xenograft models

Nude mice were obtained from Charles River Laboratories (Wilmington, MA). All manipulations were performed under sterile conditions in a laminar flow hood, in accordance with procedures approved by the DFCI Animal Care and Use Committee. A427 (5×10^6) and H1355 (5×10^6) cells were injected subcutaneously in the flanks of 6-week-old

nude mice (n = 8–10 per group). For treatment, mice were randomized into groups with similar mean tumor volumes of 100 to 150 $mm^{3.}$ Treatment began at Day 11 after implantation for A427 lines and Day 32 for H1355 lines. AZD2014 and AZD1775 was dissolved in 0.5% hydroxypropyl methylcellulose (HPMC) and administered by oral gavage once a day at 15 $mgkg^{-1}$ (AZD2014) and 40 $mgkg^{-1}$ (AZD1775).

Mice were examined every 2–3 days, and tumor length and width were measured using calipers. Tumor volume was calculated using the following formula: (length x $width^2)\pi/6$. At sacrifice, portions of tumors were snap-frozen and stored in liquid nitrogen or were fixed in 10% buffered formalin for routine histopathologic processing.

Inducible mutant KRAS-mutant lung cancer

Mouse strains harboring a conditional activating mutation (G12D) at the endogenous *KRAS* locus were induced intranasally with 5×10^7 p.f.u. *adeno-Cre* recombinase (University of Iowa adenoviral core). All experimental mice were maintained on a mixed genetic background (C57BL/6, BALB/c, and S129). Upon detection of tumor burden at approximately 14 to 16 weeks after adeno-*Cre* recombinase induction by analyzing MRI scans using 3D Slicer software, animals were randomly assigned to treatment groups (23). AZD2014 and AZD1775 was dissolved in 0.5% HPMC and administered by oral gavage once a day at 10 mg kg^{-1} (AZD2014) and 20 mg kg^{-1} (AZD1775).

Western blot analysis, antibodies and immunohistochemistry (IHC)

Whole cell extracts were lysed with lysis buffer (10 mM Tris [pH 8.0], 1% NP-40, 2 mM EDTA, 150 mM, 0.1 mM Na_3VO_4 and protease inhibitors [Roche]), resolved by SDS-PAGE and transferred to polyvinyliden fluoride membranes. Primary antibodies included: p-70S6K (Cell Signaling, #9205), p70S6 (#2708), $pCDK1^{Y15}$ (#4539), CCND1 (#2978), cPARP (#9541), LKB1 (#3080), phospho-histone H2AX (Ser 139) (20E3, #9718), β-actin (Sigma, clone AC-15), CDK1 (Santa Cruz sc-54). After blocking, membranes were incubated with relevant antibodies and probed with corresponding HRP-conjugated secondary antibodies (Cell Signaling). All blots were developed on Amersham Imager 600 (GE, Pittsburg, PA).

Tumors were fixed with 10% buffered formalin overnight and embedded in paraffin (FFPE). FFPE were cut at 4-μm thickness, dried in a 60°C oven overnight and stained with the following antibodies: TUNEL (Millipore, #S7100) and γH2AX (#9718). Ten fields per tumor section were quantified for TUNEL or γH2AX-positive cell staining with a minimum sample size of 3–8 animals per cohort.

Immunofluorescence (IF) and confocal microscopy

Cells were fixed with 4% paraformaldehyde in PBS (10 min), permeabilized with 0.1% Triton X-100 in PBS (10 min), and incubated with 0.05% SDS diluted in PBS for 5 min. After blocking in green antibody dilution buffer (Ventana Medical Systems, Oro Valley, AZ), cells were incubated overnight at 4° with followed by secondary antibodies conjugated to Alexa Fluor-488 or Alexa Fluor-647 (Invitrogen, Carlsbad, CA). The Yokogawa spinning disk confocal microscope (Zeiss USA, Thornwood, NY) was used to image the

fluorescently-stained slides. We acquired a range of 10–20 fields per treatment using Andor iQ software (Andor USA, Concord, MA) at high-power oil 100x objective.

MTS cell proliferation, colony formation and caspase activity assays

Cell proliferation/viability was evaluated by the tetrazolium dye (MTS) assay (Promega, Madison, WI). Each cell line was plated at a seeding density to give logarithmic growth over the course of the assay in a 96-well tissue culture plate. The combination indices were calculated by CalcuSyn software using the Chou-Talalay method (Biosoft, Palo Alto, CA). For colony formation assays, 0.5×10^3, 1×10^3 and 2×10^3cells were seeded on 6-well dishes and after 4–6 weeks, observed colonies were stained with crystal violet and were enumerated using ImageJ software (NIH, Bethesda). ImageJ filters scored colonies that were 50–100μm (A427) or ≥100μm (H1355) in size.

Caspase 3 and 7 activities were performed using Caspase-Glo® 3/7 assay (Promega, Madison, WI) according to manufacturer's protocol. Live time-course imaging of cells was performed and measured utilizing the IncuCyte analysis system (Essen BioSciences, Ann Arbor, MI).

Statistics

All numerical data are presented as mean ± SEM. Statistical significance was determined using one-way ANOVA with post hoc testing for comparisons of groups, including colony formation, confocal, and IHC experiments. Difference in tumor growth rates and *in vitro* growth dose curves were assessed by mixed-model two-way ANOVA. Tests that produced $P \leq 0.05$ were considered to be significant. All statistical analyses were performed with GraphPad Prism 7.0 (La Jolla, CA).

Results

Combined mTOR and WEE1 inhibition promotes anti-proliferative activity selectively in cell lines with KRAS mutations via synergistic induction of apoptotic caspase activity

We first evaluated the ability of dual inhibition of mTOR and WEE1 to inhibit cell proliferation of a panel of *KRAS*-mutant (A427, H1355, H23, H441, H2009, H358, Calu1 and H460) and *KRAS*-wildtype (HCC827, HCC4006, H1975, H3255 and H1650) NSCLC cell lines (Figure 1A–C; Supplemental Table S2–3 and Figure S1). Because patient-derived xenografts (PDX) closely mimic the molecular characteristics and heterogeneity of the original patient tumors, we further tested four cell lines cultured from early passage PDXs (PDX239, PDX277, PDX462 and PDX267) (24). Nine of the eleven cell lines achieved combination indices < 1.0, consistent with a synergistic response at nanomolar drug concentrations (Figure 1B; Supplemental Table S4). In contrast, no synergistic effects (CI>1.0) were observed in any of the *KRAS*-wildtype NSCLC cell lines treated with the drug combination, but rather single-agent activity (Figure 1C).

Further assessment of the colony growth ability of H1355 and A427 cells under long-term treatment demonstrated significantly reduced colony formation in response to dual inhibition treatments compared to monotherapy or vehicle controls (Figure 1D–F). Of note, we did not

observe significant emergence of resistant clones after six-weeks of chronic treatment. Consistent with our cell viability assays, the combination of AZD1775 and AZD2014 led to a significant increase in apoptotic caspase 3/7 activity compared to either agent alone, confirming the observed synergistic anti-tumor effects (Figure 1G **and** Supplemental Figure S2).

Combination treatment suppresses human KRAS-driven xenograft tumor growth

Given the biological implications of our *in vitro* data, we next tested the anti-tumor activity of AZD1775 and AZD2014 in human tumor xenograft mouse models. Daily oral administration of combined AZD2014 and AZD1775 treatment at clinically relevant doses significantly inhibited the rate of A427 xenograft tumor growth without toxicity ($p=0.0066$; Figure 2A and Supplemental Figure S3). At time of sacrifice, tumors treated with the combination weighed nearly 60% less than the vehicle-treated group (Figure 2B). Combination treatment for 21 days suppressed tumor progression (baseline 130±15; post-treatment 132±12 mm^3), whereas the vehicle-treated tumors progressed from 140±22 to 330±115 mm^3 (Figure 2A). We also observed significant growth suppression upon chronic administration of the combination therapy for 33 days in mice bearing H1355 xenografts (Figure 2C; $p<0.0001$). At endpoint, tumors treated with the combination weighed significantly lower on average than vehicle-treated tumors ($p=0.0087$; Figure 2D). For both models, single treatment arms showed no significant tumor reduction, suggesting lack of efficacy for the monotherapies against human KRAS-driven tumors (Figure 2B and D).

To evaluate the ability of combined therapy to induce apoptosis and DNA damage *in vivo*, cells staining positively for the DNA fragmentation marker TUNEL (Terminal deoxynucleotidyl transferase dUTP nick end labeling) and the DNA damage marker γH2AX were quantified in A427 tumors 24 hours after combined treatment and compared to vehicle controls (Figure 2E–G). We detected significantly increased numbers of TUNEL and γH2AX-positive tumor cells (2.7-fold and 2.6-fold, respectively) in the combination-treated tumors compared to controls ($p<0.0001$; Figure 2F–G). To further verify the ability of combined treatment to induce both apoptotic and DNA damage response *in vivo*, xenograft-bearing mice were treated for 6, 12, or 24 hours. Western blot analysis showed a time-dependent increase in γH2AX and levels of cleaved PARP (Figure 2H). Of note, monotherapy with either AZD2014 and AZD1775 alone failed to induce detectable accumulation of γH2AX or cleaved PARP (Figure 2H).

Mice with active KRAS-driven lung cancer show significant tumor response upon dual AZD1775 and AZD2014 therapy

To establish the translational significance of the observed synergy of WEE1 and mTOR inhibition in human NSCLC cell lines, we extended the combination treatment in well-established genetically engineered mouse models of lung adenocarcinoma having an active $KRAS^{G12D}$ mutation (25). This autochthonous, immunocompetent murine model closely recapitulates the genetic and histopathological features of human lung KRAS-driven adenocarcinoma disease and serves as a suitable clinical predictor (25). Disease course in KRAS mice was monitored by magnetic resonance imaging (MRI). Upon detection of lung tumor burden, mice were treated with vehicle, single agents, or combined AZD1775 and

AZD2014 (Figure 3A). All vehicle-treated mice showed progressive disease by the 2-week time point (PD: more than 20% increase in tumor volume compared to baseline) with tumor volume doubling at 3-weeks (Figure 3B–C). We detected significant tumor regression when mice were treated with the AZD2014 and AZD1775 combination compared to vehicle-treated mice at the two- and three-week time points (p=0.0433 and p=0.004, respectively; Figure 3B, Supplemental Figure S4). The combination therapy achieved a nearly 83% disease control rate (33% partial responses and 50% stable disease; Figure 3C) at the 3 week-time point as defined by RECIST 1.0; Partial response was defined as more than 30% decrease in tumor volume compared to baseline, while stable disease was defined as neither partial or progressive response. In contrast, 100% of tumors singly treated with either AZD1775 or AZD2014 alone progressed at nearly the same rate as vehicle-treated mice (Figure 3B–D). In fact, a few single agent-treated mice succumbed to their tumor burden before the three-week time point, emphasizing the lack of efficacy of single agent treatment alone as well as the aggressive disease course in KRAS GEM models. Furthermore, we observed no significant body weight differences between mice treated with the drug combination, suggesting that this combination did not result in treatment-related toxicity in mice (Supplemental Figure S4). Taken together, these results suggest that the combination of WEE1 and mTOR inhibition may be of potential clinical value in inducing regression of mutant KRAS-driven lung adenocarcinomas.

Dual mTOR and WEE1 inhibition leads to potent dose-dependent activation of CDK1 and compromised DNA repair by homologous recombination (HR)

Given the potent *in vitro* and *in vivo* treatment response, we next interrogated downstream effectors of WEE1 and mTOR inhibition. Combined treatment for two hours led to enhanced suppression of phosphorylation of major signaling molecules downstream of mTOR and WEE1, including $p70^{S6K}$ and CDK1 at tyrosine 15, respectively (Figure 4A). Moreover, combined treatment reduced phosphorylation of CDK1 at low nanomolar range in a dose-dependent fashion (Figure 4B).

Treatment of exponentially proliferating A427, H1355, and H23 cells for 48-hours with AZD1775 and AZD2014 led to the accumulation of γH2AX, a marker for DNA damage (Figure 4C). Consistent with this finding, we showed significantly elevated γH2AX foci in cells treated with both AZD2014 and AZD1775 (p<0.0001; Figure 4D–E). In addition to regulating the cell cycle machinery, CDK1-mediated phosphorylation of BRCA1 is also necessary for homology directed DNA repair (HR) (18). We therefore hypothesized that in addition to CDK1 activation, WEE1 inhibition would also lead to increased repair by HR in response to DNA damage from untimely mitosis. We confirmed that H23, H1355 and A427 were HR-proficient cells by assessing RAD51 focus formation upon treatment with DNA-damaging agents such as gemcitabine and etoposide (Supplemental Figure S5). Compared to vehicle-treated cells, there was significantly increased co-localization of RAD51 and γH2AX foci in response to AZD1775 treatment in NSCLC cell lines (H1355, p=0.018; A427, p<0.0001; H23, p=0.0164; Figure 4F–H). However, this enhanced level of RAD51 and γH2AX foci formation was abolished when cells were co-treated with AZD2014, suggesting disrupted repair of DNA damage may underlie potentiation of AZD1775 by AZD2014 (Figure 4F–H).

Disruption of HR repair due to potentiation of WEE1 inhibition by AZD2014 is mediated in part by reduction in cyclin D1

Activation of mTOR signaling leads to upregulation of components of the protein synthetic machinery and cap-dependent translation of crucial mRNAs for cell cycle transit, such as cyclin D1 and c-MYC (26). Cyclin D1 facilitates RAD51 recruitment to DNA repair foci (27). Therefore, we reasoned that cyclin D1-depletion may similarly sensitize cells to WEE1 inhibition. We used clustered regularly interspaced short palindromic repeats (CRISPR)-based gene editing to generate *CCND1*-deficient isogenic cell lines and lacZ-targeted sgRNA controls (Figure 5A). Knockout of *CCND1* led to significantly reduced recruitment of RAD51 to sites of DNA damage after AZD1775 treatment of H1355 and H23 cells, suggesting inefficient HR-mediated DNA repair ($p=0.0128$ and $p=0.0017$, respectively; Figure 5B–C). Additionally, we observed marked reduction of the number of co-localized RAD51 and γH2AX foci in cyclin D1-deficient cells treated with AZD2014. Importantly, AZD1775 treatment of cyclin D1-deficient cells decreased cell viability in a dose-dependent fashion compared to isogenic control cells ($p=0.0254$; Figure 5D). These results suggest that reduced cyclin D1 translation contributes to, but does not fully account for, the inhibition of HR repair mediated by AZD2014. Taken together, our results suggest that inhibition of mTOR potentiates WEE1 inhibition by abrogating compensatory activation of DNA repair, thus contributing to further DNA damage accumulation and eventual cell death (Figure 5E).

Loss of LKB1 in KRAS-mutant cell lines confers sensitivity to dual WEE1 and mTOR therapy due to impaired HR repair

KRAS activating mutations commonly co-occur with *LKB1* inactivating mutations in NSCLCs (9). We and others have demonstrated that *KRAS/LKB1*-mutant NSCLCs represent a genetically and functionally distinct subset of NSCLC (8). Interestingly, our dose-response data suggest that dual therapy was highly potent in *LKB1/KRAS*-mutant cell lines (A427, H23, H1355 and H460 cells) and previous studies have implicated LKB1 in DNA damage response (28). Hence, we investigated whether LKB1 depletion sensitizes cells to dual inhibition. We first assessed whether wild type and kinase-dead mutant forms of *LKB1*(K78I) could render LKB1-deficient RAS-driven cells resistant to dual therapy. H23 and H1355 containing empty vector (EV) constructs displayed increased sensitivity to dual therapy as evidenced by the accumulation of γH2AX protein levels and significantly increased caspase 3/7 activity compared to single-agent treatments (Figure 6A–B). When cells expressed wild type LKB1, the induction of DNA damage and apoptotic caspase activity were significantly abrogated in response to combination therapy ($p<0.0001$, Figure 6A–D, Supplemental Figure S6). In contrast, ectopic expression of dominant-negative kinase-dead mutant *LKB1*(K78I) in H23 and H1355 cells phenocopied the response of parental cells to dual therapy. Consistent with reports that LKB1 negatively regulates mTOR signaling, we found that expression of the wild type LKB1 construct in *KRAS/LKB1*-mutant cells reduced phospho-S6 activity (Supplemental Figure S7). These results confirm that LKB1 activity was indeed restored upon transfection and that *KRAS/LKB1*-mutant cells confer hyperactive mTOR signaling. Despite the reduction in mTOR signaling afforded by expression of wild type LKB1, these cells displayed effective HR repair as observed by restored RAD51 and γH2AX foci upon dual treatment (Figure 6C–F, Supplemental Figure S8). Indeed, LKB1 can stimulate DNA repair by modulating BRCA1 levels (28). In contrast,

LKB1-deficient cells may be more reliant on mTOR activity to simulate repair and therefore may be vulnerable to AZD2014 treatment after AZ1775-mediated DNA damage.

Discussion

Despite the development of agents targeting specific genetic subsets of NSCLCs, KRAS-driven lung cancer presently remains “untargetable” and is therefore a highly lethal disease. Exploiting synthetic lethal interactions to selectively target *KRAS*-mutant lung cancers is warranted. Here, we provide mechanistic evidence that simultaneous inhibition of WEE1 and mTOR signaling allows for more complete disruption of compensatory pathways, resulting in cytotoxic synergy in *KRAS*-driven NSCLC cell lines and PDX-derived cell lines that more closely mimic the heterogeneity of patient tumors. Importantly, we demonstrated anti-tumor efficacy upon combined treatment with inhibitors at clinically relevant doses in *KRAS*-GEM models that closely recapitulate human disease.

Activation of KRAS or inhibition of WEE1 deregulates CDK activity and leads to replication stress and subsequent DNA damage (29, 30). Initial preclinical studies on AZD1775 focused on chemo-potentiation based on the rationale that disrupted cell-cycle checkpoints would allow for untimely entry into cell division with unrepaired DNA lesions, resulting in cell death (19, 31, 32). However, more recent observations suggest that the mechanism of AZD1775 cytotoxicity is primarily through DNA damage rather than premature mitosis, consistent with our observations of increased γH2AX-positive cells and apoptotic activity upon single-agent treatment in KRAS-mutant cells (33, 34). Earlier studies have focused on p53-deficient tumors for WEE1 inhibition, based on the reasoning that cells defective in the G1 checkpoint as a result of p53 loss-of-function would be dependent on the G2 checkpoint survival. Here we observed similar cytotoxic profiles to dual therapy among A427 and H460 cells bearing wild type *TP53* and cells containing mutant *TP53* (H1355 and H23), suggesting that the cytotoxic synergy is independent of p53 status (31, 34).

In agreement with previous studies implicating CDK1 in DNA repair, we show here that WEE1 inhibition not only increased CDK1 activity in a dose-dependent manner, but also significantly induced HR repair to compensate for the resultant DNA damage (18). Johnson *et al.* previously showed that CDK1-mediated phosphorylation of BRCA1 is required for HR repair and CDK1-depleted cancer cells are HR-defective and sensitized to PARP inhibition both *in vitro* and *in vivo* (18). This finding partly explains why single-agent treatment may lack long-term efficiency as cancer cells acquire a CDK1-mediated bypass response. Based on our data, coupling AZD1775 to agents that compromise DNA repair would exacerbate cancer cell killing. Indeed, combined inhibition of checkpoint kinase 1 (CHK1), a kinase implicated in the DNA damage response, and WEE1 has shown therapeutic efficacy in neuroblastoma (35). However, a prior study demonstrated that forced activation of CDK1 via WEE1 inhibition can also impair HR repair in breast cancer cell lines, suggesting that the effects of AZD1775 may also be genotype and cell-type dependent (36). Furthermore, recent studies have revealed a novel role of WEE1 in the maintenance of nucleotide (dNTP) pools through regulation of ribonucleotide reductase subunit 2, RRM2 (30). Pfister *et al.* identified that loss of methyltransferase SETD2 is synthetically lethal with loss of WEE1 in cancer cells due to dNTP starvation via RRM2 deregulation (30). Taken together, these data reveal

alternative mechanisms by which WEE1 inhibition can lead to DNA damage. It is therefore possible that TORC1/2 inhibitor-mediated reduction in DNA repair may lead to a synthetic lethal interaction in other cell types besides NSCLC harboring *KRAS* mutation, constituting a direction for future studies.

Several reports have indicated that cell cycle regulator proteins directly control proteins in DNA repair pathways (27, 37). Given that cyclin D1 facilities RAD51 recruitment to DNA repair foci and is a downstream target of mTOR signaling, we asked whether depletion of cyclin D1 expression was sufficient to override AZD2014-mediated potentiation to AZD1775 (27, 38). We showed that AZD1775 treatment was insufficient to induce HR repair in CRISPR *CCND1*-deficient cells compared to sgLacZ-control cells. Moreover, AZD2014 treatment further reduced levels of RAD51 and γH2AX foci formation in *CCND1*-deficient cells compared to control cells, confirming that mTOR signaling is necessary for proper HR repair in KRAS-mutant cells. Although cell viability assays showed that *CCND1* depletion was significantly more sensitive to AZD1775 monotherapy than control cells, this response was less potent than the dual inhibition response. Previous studies have shown that mTOR inhibitors suppress HR repair by deregulating expression of a key histone methyltransferase, SUV39H1, in BRCA1-proficient breast cancer cells (39). Shen *et al.* demonstrated that mTOR positively regulates Fanconi anemia group D2 protein, FANCD2, which is recruited to DNA interstrand crosslinks required for proper DNA repair (40). These studies suggest that mTOR elicits multiple cascades linked to cellular DNA repair machinery (41, 42). Therefore, we postulate that other mTOR downstream effectors may also contribute to HR repair. Taken together, our data show that DNA repair is a major target of the synthetic lethal interaction between WEE1 and mTOR inhibition.

LKB1 is a multifaceted tumor suppressor implicated in a variety of cellular processes including signal transduction, energy sensing, cell polarity and dNTP metabolism (43–46). Recently, Gupta *et al.* showed a role for LKB1 in preserving genome integrity by stimulating the expression of BRCA1 to mediate DNA damage response pathways (28). LKB1 has been found to post-transcriptionally stabilize BRCA1 mRNA by inhibiting the cytoplasmic localization of the RNA-binding protein, Hu antigen R (HuR). Here, we demonstrated that ectopic expression of wild type *LKB1* in *KRAS*-mutant cells bearing LKB1 inactivating mutations prevented accumulation of DNA damage after AZD1775 monotherapy treatment. Additionally, wild type LKB1 restoration also prevented reduced HR repair after AZD2014 exposure and therefore also prevented the accumulation of DNA damage after dual therapy. Conversely, expression of a kinase-dead LKB1 mutant phenocopied the response of LKB-mutant cells to dual therapy, confirming that LKB1 activity is necessary for proper DNA repair. Corroborating this observation, a recent Phase I study of single-agent AZD1775 in adult patients with refractory solid tumors demonstrated objective responses in two patients carrying *BRCA1* mutations, supporting the notion that LKB1 plays a role in the response to DNA damage induced by WEE1 inhibition (17).

Consistent with prior studies that reported increased sensitivity to MAPK and mTOR signaling inhibition in *KRAS/LKB1*-mutant subsets of lung cancers, we observed that *KRAS/LKB1*-mutants conferred hyperactivation of mTOR signaling (47) (Supplemental Figure S4). LKB1-deficient cells would be unable to stimulate BRCA1 expression after

WEE1 inhibitor-mediated DNA damage and may be very reliant on hyperactivated mTOR activity to stimulate DNA repair, explaining the particularly high degree of sensitivity of *KRAS/LKB1*-mutant cells to dual therapy. Such cells would be expected to be hypersensitive to mTOR inhibition. Additionally, HuR localization of which is affected by LKB1, also regulates levels of WEE1 (28, 48). We speculate that loss of LKB1 may elicit elevated WEE1 activity, which may depend on AZD1775 to override signals in RAS-mutant cells (28, 48). Based on these studies, it would be interesting to comprehensively examine the role of other HuR downstream targets to understand their role in mediating LKB1-loss-induced sensitization to DNA damage via dual therapy.

Our *in vitro* observations were translated in xenograft models, where dual therapy resulted in the accumulation of both γH2AX and TUNEL-positive staining in tumors. We also evaluated treatment response in mice with lung-specific conditional activation of $KRAS^{G12D}$ mutations that developed aggressive lung adenocarcinomas (25). The WEE1 and mTOR inhibitor combination induced regression and disease stabilization over 2–3 weeks of treatment in established tumors. Interestingly, the combinatorial treatment was successful *in vivo* in an LKB1-proficient setting, suggesting that induction of HR mediated by LKB1 *in vivo* may not be as profound as that observed in *in vitro* models studied here or in other cell systems (40). It will be of interest to determine whether combinatorial effects are even more profound in LKB1-deficient mouse models. Notably, we did not detect any drug-related toxicity during the course of 3-week treatment on mice, consistent with a recent Phase I study showing AZD1775 tolerability and safety as monotherapy and in combination with standard chemotherapy in 202 patients (49).

In summary, the present study is the first to show that AZD2014 potentiates AZD1775 by abrogating compensatory activation of HR repair, resulting in cytotoxic synergism. Considering the absence of targeted therapies available for KRAS-driven NSCLC, dual inhibition of mTOR and WEE1 should be investigated as a potential strategy. Additionally, since tumors harboring concomitant KRAS activation and LKB1 loss are among the most highly aggressive, combined mTOR and WEE1 inhibition may be particularly compelling for this lung cancer subset.

Supplementary Material

Refer to Web version on PubMed Central for supplementary material.

Acknowledgments

Financial support: Financial support: This work was supported by the National Cancer Institute (R01CA195740, CA163896, CA166480, CA122794, and CA140594), the Thoracic Foundation (K.K. Wong), the Gross-Loh Family Fund for Lung Cancer Research, and the Susan Spooner Family Lung Cancer Research Fund at Dana-Farber Cancer Institute (K.K. Wong). K.K. Wong supported by a Stand Up To Cancer – American Cancer Society Lung Cancer Dream Team Translational Research Grant (Grant Number: SU2C-AACR-DT1715). Stand Up To Cancer is a program of the Entertainment Industry Foundation. Research grants are administered by the American Association for Cancer Research, the Scientific Partner of SU2C.

The authors thank Mei Zhang for help with immunohistochemistry work, Yanxi Zhang for technical animal assistance and Dr. Shunsuke Kitajima, Dr. Nhu-An Pham, and Belfer Institute for providing PDX and NSCLC cell lines. We also thank AstraZeneca for making AZD2014 and AZD1775 available for this study and Belfer Institute and Pinar Eser for making the IncuCyte system available to us.

References

1. Siegel RL, Miller KD, Jemal A. Cancer statistics, 2015. CA: a cancer journal for clinicians. 2015; 65:5–29. [PubMed: 25559415]
2. Global Cancer Facts & Figures. 3. American Cancer Society; 2015.
3. Stephen AG, Esposito D, Bagni RK, McCormick F. Dragging ras back in the ring. Cancer cell. 2014; 25:272–81. [PubMed: 24651010]
4. Ostrem JM, Peters U, Sos ML, Wells JA, Shokat KM. K-Ras(G12C) inhibitors allosterically control GTP affinity and effector interactions. Nature. 2013; 503:548–51. [PubMed: 24256730]
5. Chong CR, Janne PA. The quest to overcome resistance to EGFR-targeted therapies in cancer. Nature medicine. 2013; 19:1389–400.
6. Camidge DR, Bang YJ, Kwak EL, Iafrate AJ, Varella-Garcia M, Fox SB, et al. Activity and safety of crizotinib in patients with ALK-positive non-small-cell lung cancer: updated results from a phase 1 study. The Lancet Oncology. 2012; 13:1011–9. [PubMed: 22954507]
7. Stinchcombe TE, Johnson GL. MEK inhibition in non-small cell lung cancer. Lung cancer (Amsterdam, Netherlands). 2014; 86:121–5.
8. Skoulidis F, Byers LA, Diao L, Papadimitrakopoulou VA, Tong P, Izzo J, et al. Co-occurring genomic alterations define major subsets of KRAS-mutant lung adenocarcinoma with distinct biology, immune profiles, and therapeutic vulnerabilities. Cancer discovery. 2015; 5:860–77. [PubMed: 26069186]
9. Chen Z, Cheng K, Walton Z, Wang Y, Ebi H, Shimamura T, et al. A murine lung cancer co-clinical trial identifies genetic modifiers of therapeutic response. Nature. 2012; 483:613–7. [PubMed: 22425996]
10. Herter-Sprie GS, Koyama S, Korideck H, Hai J, Deng J, Li YY, et al. Synergy of radiotherapy and PD-1 blockade in Kras-mutant lung cancer. JCI insight. 2016; 1:e87415. [PubMed: 27699275]
11. Weisberg E, Nonami A, Chen Z, Liu F, Zhang J, Sattler M, et al. Identification of Wee1 as a novel therapeutic target for mutant RAS-driven acute leukemia and other malignancies. Leukemia. 2015; 29:27–37. [PubMed: 24791855]
12. McCubrey JA, Steelman LS, Chappell WH, Abrams SL, Franklin RA, Montalto G, et al. Ras/Raf/MEK/ERK and PI3K/PTEN/Akt/mTOR cascade inhibitors: how mutations can result in therapy resistance and how to overcome resistance. Oncotarget. 2012; 3:1068–111. [PubMed: 23085539]
13. Chen H, Ma Z, Vanderwaal RP, Feng Z, Gonzalez-Suarez I, Wang S, et al. The mTOR inhibitor rapamycin suppresses DNA double-strand break repair. Radiation research. 2011; 175:214–24. [PubMed: 21268715]
14. Guichard SM, Curwen J, Bihani T, D'Cruz CM, Yates JW, Grondine M, et al. AZD2014, an Inhibitor of mTORC1 and mTORC2, Is Highly Effective in ER+ Breast Cancer When Administered Using Intermittent or Continuous Schedules. Molecular cancer therapeutics. 2015; 14:2508–18. [PubMed: 26358751]
15. Powles T, Wheater M, Din O, Geldart T, Boleti E, Stockdale A, et al. A Randomised Phase 2 Study of AZD2014 Versus Everolimus in Patients with VEGF-Refractory Metastatic Clear Cell Renal Cancer. European urology. 2016; 69:450–6. [PubMed: 26364551]
16. Parker LL, Piwnica-Worms H. Inactivation of the p34cdc2-cyclin B complex by the human WEE1 tyrosine kinase. Science (New York, NY). 1992; 257:1955–7.
17. Do K, Wilsker D, Ji J, Zlott J, Freshwater T, Kinders RJ, et al. Phase I Study of Single-Agent AZD1775 (MK-1775), a Wee1 Kinase Inhibitor, in Patients With Refractory Solid Tumors. Journal of clinical oncology: official journal of the American Society of Clinical Oncology. 2015; 33:3409–15. [PubMed: 25964244]
18. Johnson N, Li YC, Walton ZE, Cheng KA, Li D, Rodig SJ, et al. Compromised CDK1 activity sensitizes BRCA-proficient cancers to PARP inhibition. Nature medicine. 2011; 17:875–82.
19. Rajeshkumar NV, De Oliveira E, Ottenhof N, Watters J, Brooks D, Demuth T, et al. MK-1775, a potent Wee1 inhibitor, synergizes with gemcitabine to achieve tumor regressions, selectively in p53-deficient pancreatic cancer xenografts. Clinical cancer research: an official journal of the American Association for Cancer Research. 2011; 17:2799–806. [PubMed: 21389100]

20. John T, Kohler D, Pintilie M, Yanagawa N, Pham NA, Li M, et al. The ability to form primary tumor xenografts is predictive of increased risk of disease recurrence in early-stage non-small cell lung cancer. Clinical cancer research: an official journal of the American Association for Cancer Research. 2011; 17:134–41. [PubMed: 21081655]
21. Hai J, Sakashita S, Allo G, Ludkovski O, Ng C, Shepherd FA, et al. Inhibiting MDM2-p53 Interaction Suppresses Tumor Growth in Patient-Derived Non-Small Cell Lung Cancer Xenograft Models. Journal of thoracic oncology: official publication of the International Association for the Study of Lung Cancer. 2015; 10:1172–80.
22. Hai J, Zhu CQ, Wang T, Organ SL, Shepherd FA, Tsao MS. TRIM14 is a Putative Tumor Suppressor and Regulator of Innate Immune Response in Non-Small Cell Lung Cancer. Scientific reports. 2017; 7:39692. [PubMed: 28059079]
23. Fedorov A, Beichel R, Kalpathy-Cramer J, Finet J, Fillion-Robin JC, Pujol S, et al. 3D Slicer as an image computing platform for the Quantitative Imaging Network. Magnetic resonance imaging. 2012; 30:1323–41. [PubMed: 22770690]
24. Wang D, Pham NA, Tong J, Sakashita S, Allo G, Kim L, et al. Molecular heterogeneity of non-small cell lung carcinoma patient-derived xenografts closely reflect their primary tumors. International journal of cancer. 2017; 140:662–73. [PubMed: 27750381]
25. Sweet-Cordero A, Mukherjee S, Subramanian A, You H, Roix JJ, Ladd-Acosta C, et al. An oncogenic KRAS2 expression signature identified by cross-species gene-expression analysis. Nature genetics. 2005; 37:48–55. [PubMed: 15608639]
26. Gera JF, Mellinghoff IK, Shi Y, Rettig MB, Tran C, Hsu JH, et al. AKT activity determines sensitivity to mammalian target of rapamycin (mTOR) inhibitors by regulating cyclin D1 and c-myc expression. The Journal of biological chemistry. 2004; 279:2737–46. [PubMed: 14576155]
27. Chalermrujinanant C, Michowski W, Sittithumcharee G, Esashi F, Jirawatnotai S. Cyclin D1 promotes BRCA2-Rad51 interaction by restricting cyclin A/B-dependent BRCA2 phosphorylation. Oncogene. 2016; 35:2815–23. [PubMed: 26387543]
28. Gupta R, Liu AY, Glazer PM, Wajapeyee N. LKB1 preserves genome integrity by stimulating BRCA1 expression. Nucleic acids research. 2015; 43:259–71. [PubMed: 25488815]
29. Minocherhomji S, Ying S, Bjerregaard VA, Bursomanno S, Aleliunaite A, Wu W, et al. Replication stress activates DNA repair synthesis in mitosis. Nature. 2015; 528:286–90. [PubMed: 26633632]
30. Pfister SX, Markkanen E, Jiang Y, Sarkar S, Woodcock M, Orlando G, et al. Inhibiting WEE1 Selectively Kills Histone H3K36me3-Deficient Cancers by dNTP Starvation. Cancer cell. 2015; 28:557–68. [PubMed: 26602815]
31. Hirai H, Arai T, Okada M, Nishibata T, Kobayashi M, Sakai N, et al. MK-1775, a small molecule Wee1 inhibitor, enhances anti-tumor efficacy of various DNA-damaging agents, including 5-fluorouracil. Cancer biology & therapy. 2010; 9:514–22. [PubMed: 20107315]
32. Hirai H, Iwasawa Y, Okada M, Arai T, Nishibata T, Kobayashi M, et al. Small-molecule inhibition of Wee1 kinase by MK-1775 selectively sensitizes p53-deficient tumor cells to DNA-damaging agents. Molecular cancer therapeutics. 2009; 8:2992–3000. [PubMed: 19887545]
33. Guertin AD, Li J, Liu Y, Hurd MS, Schuller AG, Long B, et al. Preclinical evaluation of the WEE1 inhibitor MK-1775 as single-agent anticancer therapy. Molecular cancer therapeutics. 2013; 12:1442–52. [PubMed: 23699655]
34. Kreahling JM, Gemmer JY, Reed D, Letson D, Bui M, Altiok S. MK1775, a selective Wee1 inhibitor, shows single-agent antitumor activity against sarcoma cells. Molecular cancer therapeutics. 2012; 11:174–82. [PubMed: 22084170]
35. Russell MR, Levin K, Rader J, Belcastro L, Li Y, Martinez D, et al. Combination therapy targeting the Chk1 and Wee1 kinases shows therapeutic efficacy in neuroblastoma. Cancer research. 2013; 73:776–84. [PubMed: 23135916]
36. Krajewska M, Heijink AM, Bisselink YJ, Seinstra RI, Sillje HH, de Vries EG, et al. Forced activation of Cdk1 via wee1 inhibition impairs homologous recombination. Oncogene. 2013; 32:3001–8. [PubMed: 22797065]
37. Esashi F, Christ N, Gannon J, Liu Y, Hunt T, Jasin M, et al. CDK-dependent phosphorylation of BRCA2 as a regulatory mechanism for recombinational repair. Nature. 2005; 434:598–604. [PubMed: 15800615]

38. Takuwa N, Fukui Y, Takuwa Y. Cyclin D1 expression mediated by phosphatidylinositol 3-kinase through mTOR-p70(S6K)-independent signaling in growth factor-stimulated NIH 3T3 fibroblasts. Molecular and cellular biology. 1999; 19:1346–58. [PubMed: 9891068]

39. Fritsch L, Robin P, Mathieu JR, Souidi M, Hinaux H, Rougeulle C, et al. A subset of the histone H3 lysine 9 methyltransferases Suv39h1, G9a, GLP, and SETDB1 participate in a multimeric complex. Molecular cell. 2010; 37:46–56. [PubMed: 20129054]

40. Shen C, Oswald D, Phelps D, Cam H, Pelloski CE, Pang Q, et al. Regulation of FANCD2 by the mTOR pathway contributes to the resistance of cancer cells to DNA double-strand breaks. Cancer research. 2013; 73:3393–401. [PubMed: 23633493]

41. Mo W, Liu Q, Lin CC, Dai H, Peng Y, Liang Y, et al. mTOR Inhibitors Suppress Homologous Recombination Repair and Synergize with PARP Inhibitors via Regulating SUV39H1 in BRCA-Proficient Triple-Negative Breast Cancer. Clinical cancer research: an official journal of the American Association for Cancer Research. 2016; 22:1699–712. [PubMed: 26546619]

42. Liang CC, Li Z, Lopez-Martinez D, Nicholson WV, Venien-Bryan C, Cohn MA. The FANCD2-FANCI complex is recruited to DNA interstrand crosslinks before monoubiquitination of FANCD2. Nature communications. 2016; 7:12124.

43. Liang J, Shao SH, Xu ZX, Hennessy B, Ding Z, Larrea M, et al. The energy sensing LKB1-AMPK pathway regulates p27(kip1) phosphorylation mediating the decision to enter autophagy or apoptosis. Nature cell biology. 2007; 9:218–24. [PubMed: 17237771]

44. Liu Y, Marks K, Cowley GS, Carretero J, Liu Q, Nieland TJ, et al. Metabolic and functional genomic studies identify deoxythymidylate kinase as a target in LKB1-mutant lung cancer. Cancer discovery. 2013; 3:870–9. [PubMed: 23715154]

45. Kottakis F, Nicolay BN, Roumane A, Karnik R, Gu H, Nagle JM, et al. LKB1 loss links serine metabolism to DNA methylation and tumorigenesis. Nature. 2016; 539:390–5. [PubMed: 27799657]

46. Nakano A, Takashima S. LKB1 and AMP-activated protein kinase: regulators of cell polarity. Genes to cells: devoted to molecular & cellular mechanisms. 2012; 17:737–47. [PubMed: 22892070]

47. Mahoney CL, Choudhury B, Davies H, Edkins S, Greenman C, Haaften G, et al. LKB1/KRAS mutant lung cancers constitute a genetic subset of NSCLC with increased sensitivity to MAPK and mTOR signalling inhibition. British journal of cancer. 2009; 100:370–5. [PubMed: 19165201]

48. Lal S, Burkhart RA, Beeharry N, Bhattacharjee V, Londin ER, Cozzitorto JA, et al. HuR posttranscriptionally regulates WEE1: implications for the DNA damage response in pancreatic cancer cells. Cancer research. 2014; 74:1128–40. [PubMed: 24536047]

49. Leijen S, van Geel RM, Pavlick AC, Tibes R, Rosen L, Razak AR, et al. Phase I Study Evaluating WEE1 Inhibitor AZD1775 As Monotherapy and in Combination With Gemcitabine, Cisplatin, or Carboplatin in Patients With Advanced Solid Tumors. Journal of clinical oncology: official journal of the American Society of Clinical Oncology. 2016

Translational relevance

Considering the absence of targeted therapies for KRAS-driven cancers, the identification of combinatorial therapies remains an area of great clinical need. Here, we provide mechanistic rationale for combining mTOR and WEE1 inhibition to selectively target *KRAS*-mutant NSCLCs. We demonstrate for the first time that inhibition of mTOR potentiates WEE1 inhibition by mitigating compensatory activation of DNA repair by homologous recombination, resulting in cytotoxic synergism. Thus, dual inhibition of mTOR and WEE1 in *KRAS*-driven NSCLCs presents a promising approach when targeted therapies remain elusive in this patient population.

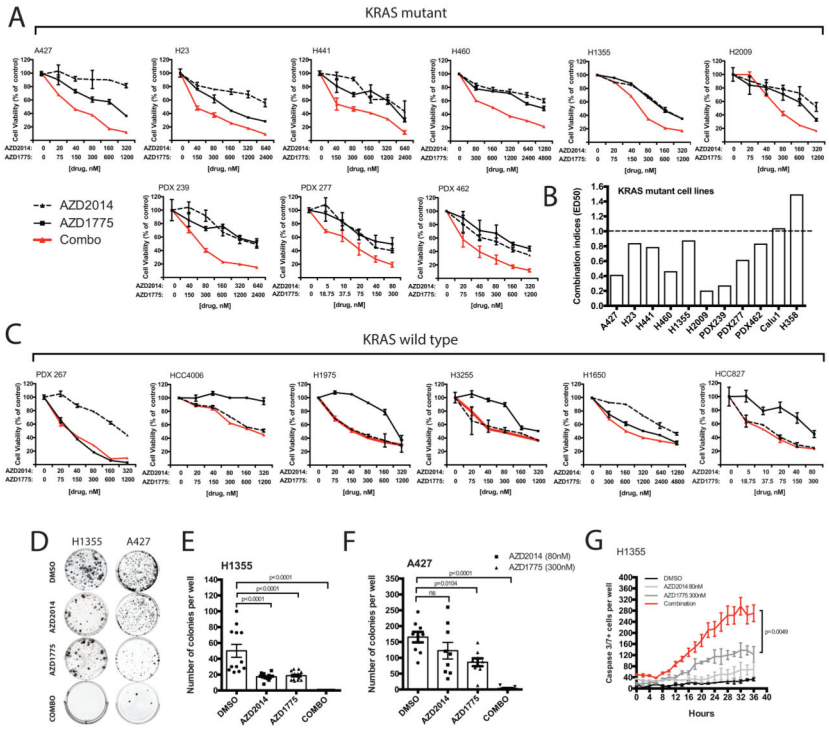

Figure 1. Combined mTOR and WEE1 inhibition promotes anti-proliferative activity selectively in cell lines with KRAS mutations via synergistic induction of apoptotic caspase activity

(A–C) Dose-response curves were measured by MTS assay. (A) *KRAS*-mutant exponentially growing cell lines were incubated with either single agents or dual therapy for three days. (B) CalcuSyn combination indices (CI) were derived from six-point concentration proliferation experiments. The cutoff for additive effect (CI: 1) is marked by a dashed line. (C) Dose-response curves of *KRAS*-wildtype cell lines treated for three days with either single agents or combined agents. (D) Representative images of H1355 and A427 colony formation, untreated or treated with either AZD2014 (80nM), AZD1775 (300nM) or in combination for four weeks. (E–F) Mean number of colonies formed after treating (E) H1355 (≥100μm) and (F) A427 (50–100μm) cells for four weeks. (G) Live time-course imaging was used to detect the mean number of caspase3/7-positive cells induced under treatment. Each time point represents 3 wells in duplicates (n=6) (PDX: patient-derived xenografted cell lines; ns: not significant, p>0.05).

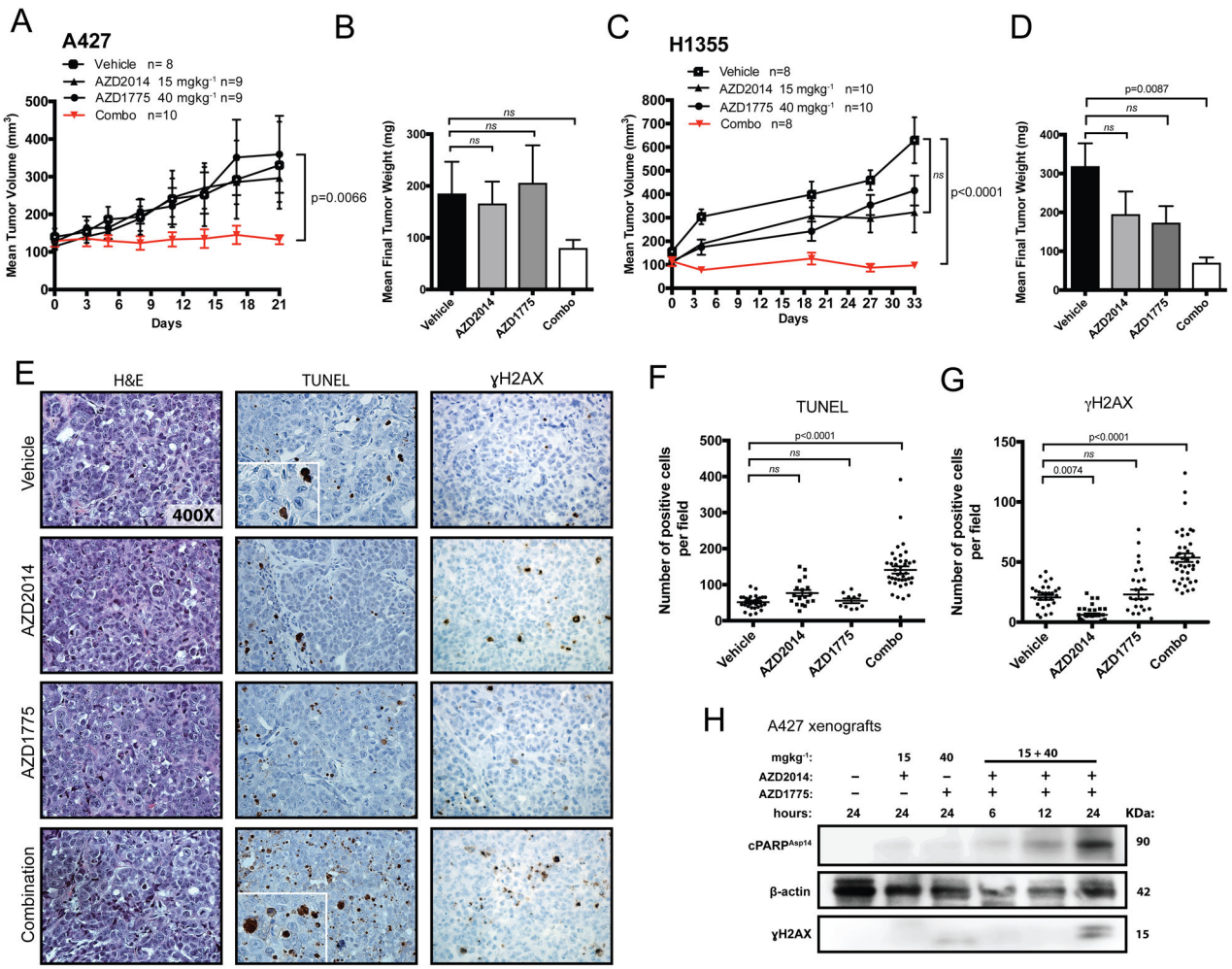

Figure 2. Combination treatment suppresses human KRAS-driven tumor xenografted growth

(A–D) Effect of single agent and dual treatment on tumor growth of A427 (A) and H1355 (C) cells in nude mice dosed daily (QD) at 15 mgkg^{-1} (AZD2014) and 40 mgkg^{-1} (AZD1775). (B–D) Final A427- and H1355-treated tumor weights at time of sacrifice compared to vehicle-treated tumors. The data points represent the averages of 8 to 10 tumors per treatment group. The p-values were calculated using mixed model ANOVA testing for tumor growth rates and ANOVA with post Tukey testing for final tumor weights. (E) Representative histologic sections of xenografts from A427 tumors were immunostained with TUNEL and γH2AX. (F–G) The percentage of positive TUNEL (F) and γH2AX (G) cells in A427 tumor sections were scored at 10 high-power fields (n=3–4/group). The p-values were calculated based on ANOVA with Tukey post testing. (H) Western blot analysis of changes in protein levels of γH2AX and cleaved PARP expression in A427 tumors treated for indicated times (ns: not significant, p>0.05).

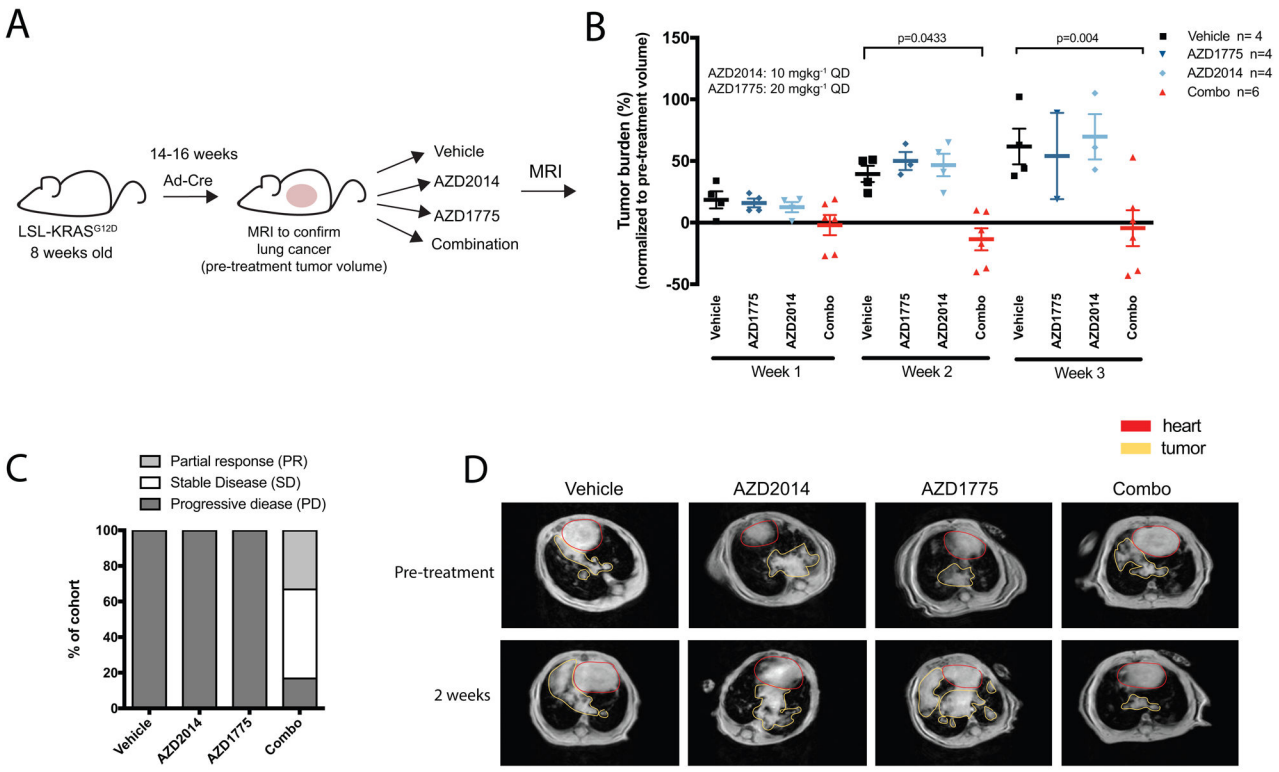

Figure 3. Mice with active KRAS-driven lung cancer show significant tumor response upon dual AZD1775 and AZD2014 therapy

(A) Upon detection of tumor burden by MRI at approximately 14–16 weeks after *adeno-Cre* recombinase induction, mice were randomized to treatment arms. Mice were dosed daily (QD) at 10 mgkg^{-1} (AZD2014) and 20 mgkg^{-1} (AZD1775). MRI was performed weekly in all treatment cohorts. (B) Tumor volume changes (%) according to MRI quantification in vehicle-treated (control), AZD2014-treated, AZD1775-treated and combined therapy mice at one to three weeks as normalized to pre-treatment (week 0) tumor volume. Data are shown as individual values for tumor volume change with horizontal line representing the mean. A few single agent-treated mice succumbed to their tumor burden before the three-week time point, emphasizing the lack of efficacy of single agent treatment alone. (C) Treatment response as divided into progressive disease, stable disease, and partial response groups in mice treated with vehicle (control), single-agent alone and combination. Data is shown as percent of total mice in respective treatment cohorts. (D) Representative MRIs of thorax region of mice in each treatment group at pretreatment and week 2.

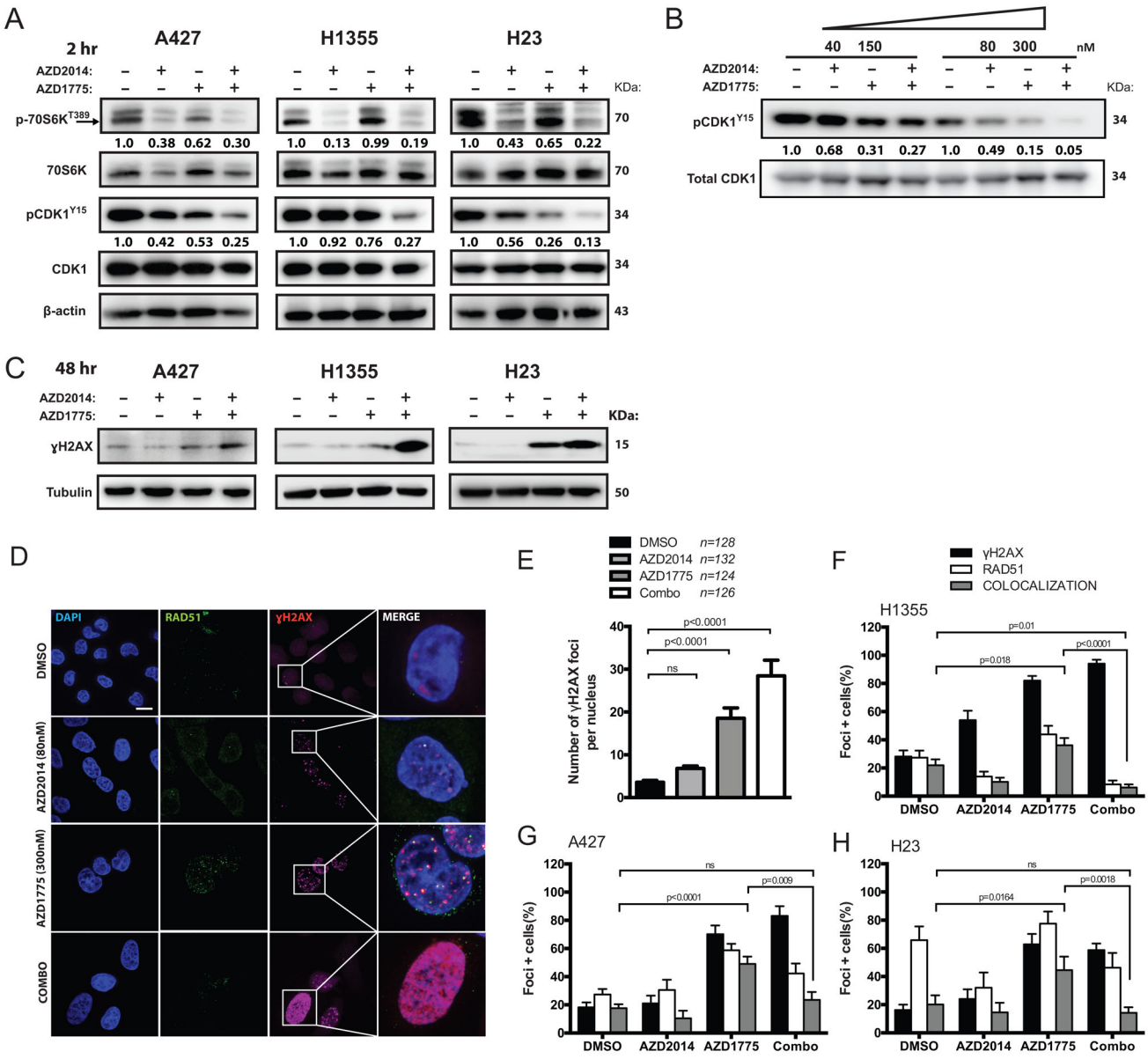

Figure 4. Dual mTOR and WEE1 inhibition leads to potent dose-dependent activation of CDK1 and compromised DNA repair by HR

(A) Representative western blots showing protein levels of downstream target engagement (CDK1, p70S6K and γH2AX) in A427, H1355, and H23 cells treated for two hours with vehicle (DMSO), AZD2014 (80nM), AZD1775 (300nM) or combination. Relative levels of optical density of phospho-protein bands were normalized to the total protein expressions and shown below. (B) Dual therapy dose dependently enhanced dephosphorylation of CDK1 at tyrosine 15 in H23 cells after two hours of treatment. Corresponding pCDK protein quantifications were normalized to total CDK1 levels. (C) Representative western blots showing γH2AX protein levels in A427, H1355, and H23 cells treated with indicated drugs for 48-hours. (D) Detection of RAD51, γH2AX and DAPI in H1355 cells by immunofluorescence after 48-hour treatment with indicated drugs. Representative foci-

containing cells at high-power magnification (100x oil) are shown. Scale bar: 10μm. (E) Mean number of γH2AX-focus per H1355 nuclei after 48 hours treatment with either 80nM AZD2014, 300nM AZD1775 or both. Over 120 nuclei were analyzed over three experiments. (F–H) Mean number of cells containing ≥ five γH2AX and ≥ one RAD51 foci by immunofluorescence in H1355 (F), A427 (G) and H23 (H) cells over three experiments. Cells were treated either 80nM AZD2014, 300nM AZD1775 or in combination after 48-hours. (ns: not significant)

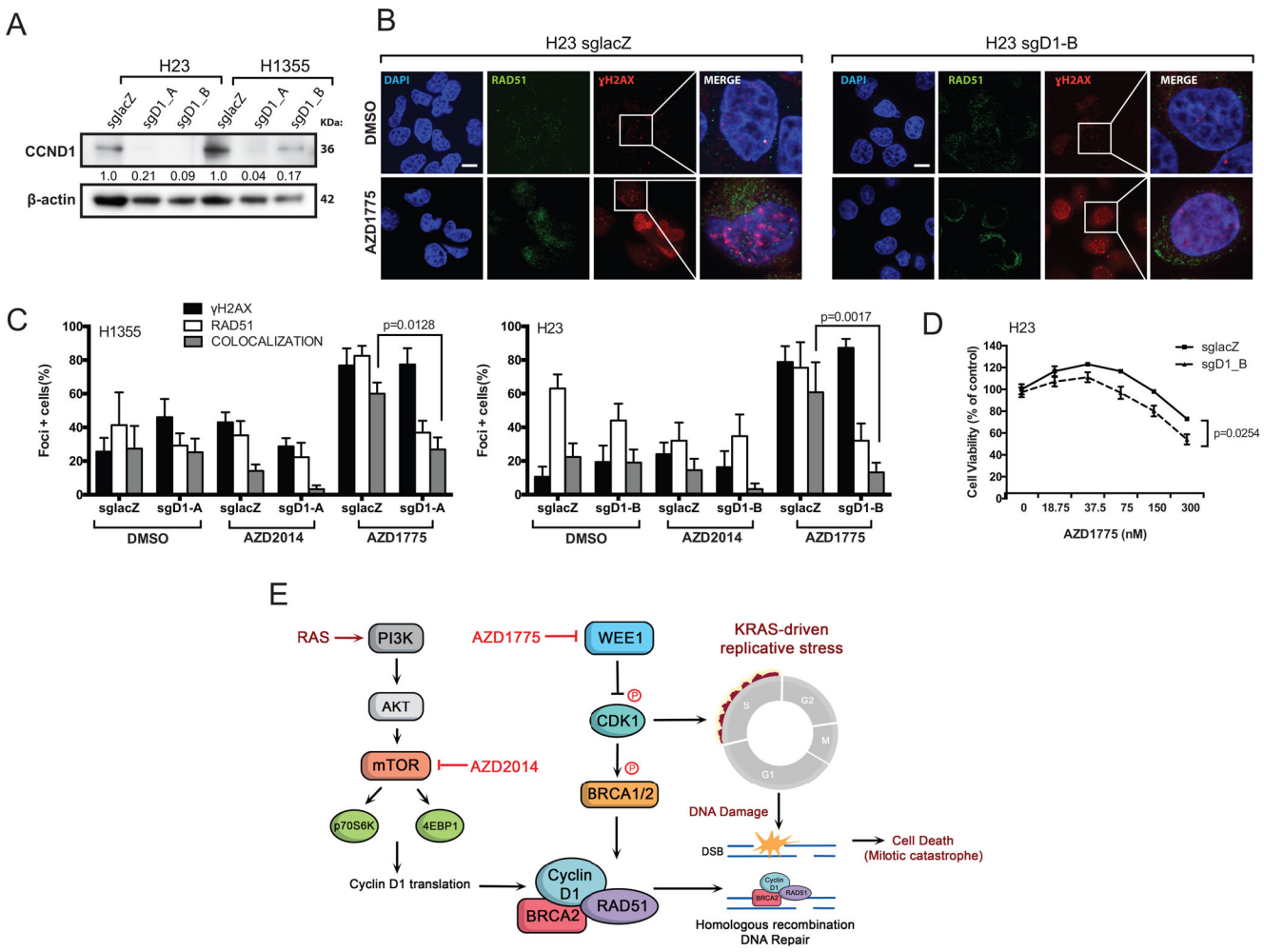

Figure 5. HR repair pathways partially mediates potentiation of WEE1 inhibition by AZD2014

(A) Western blots demonstrate CCND1 protein knockdown after treatment with sgRNAs targeting either LacZ (control) or CCND1 (2 different target sites) in H23 and H1355 cells. Corresponding CCND1 protein quantifications were normalized to β-actin loading control. (B) Detection of RAD51, γ-H2AX and DAPI by immunofluorescence in H23 cells expressing sgRNA targeting CCND1, untreated or treated with AZD1775 at 300nM. Representative foci-containing cells are shown at high power magnification (100x). Scale bar: 10μm. (C) Mean number of cells containing ≥ five γ-H2AX and RAD51 foci by immunofluorescence in H1355 (left panel) and A427 (right panel) cells treated with either DMSO, AZD2015 (80nM), or AZD1775 (300nM) for 48 hours. (D) Dose-response curves of H23 cells expressing either sgCCND1 or control guide, untreated or treated with 300nM AZD1775 for three days. Significance was calculated for H23-sgCCND1 drug response versus control cells using ANOVA-mixed model testing. (E) A simplified model showing cross-talk and compensation by mTOR and WEE1-mediated regulation of DNA repair by HR. RAS activation of PI3K/AKT/mTOR pathway phosphorylates p70S6K and 4E-BP1, which promote cyclin D1 translation. WEE1 inhibits CDK1, which can phosphorylate BRCA1/2 to promote RAD51 focus formation necessary for HR repair. *KRAS*-driven

cancers undergo replicative stress and are vulnerable to DNA damage accumulation when cell cycle checkpoints are compromised.

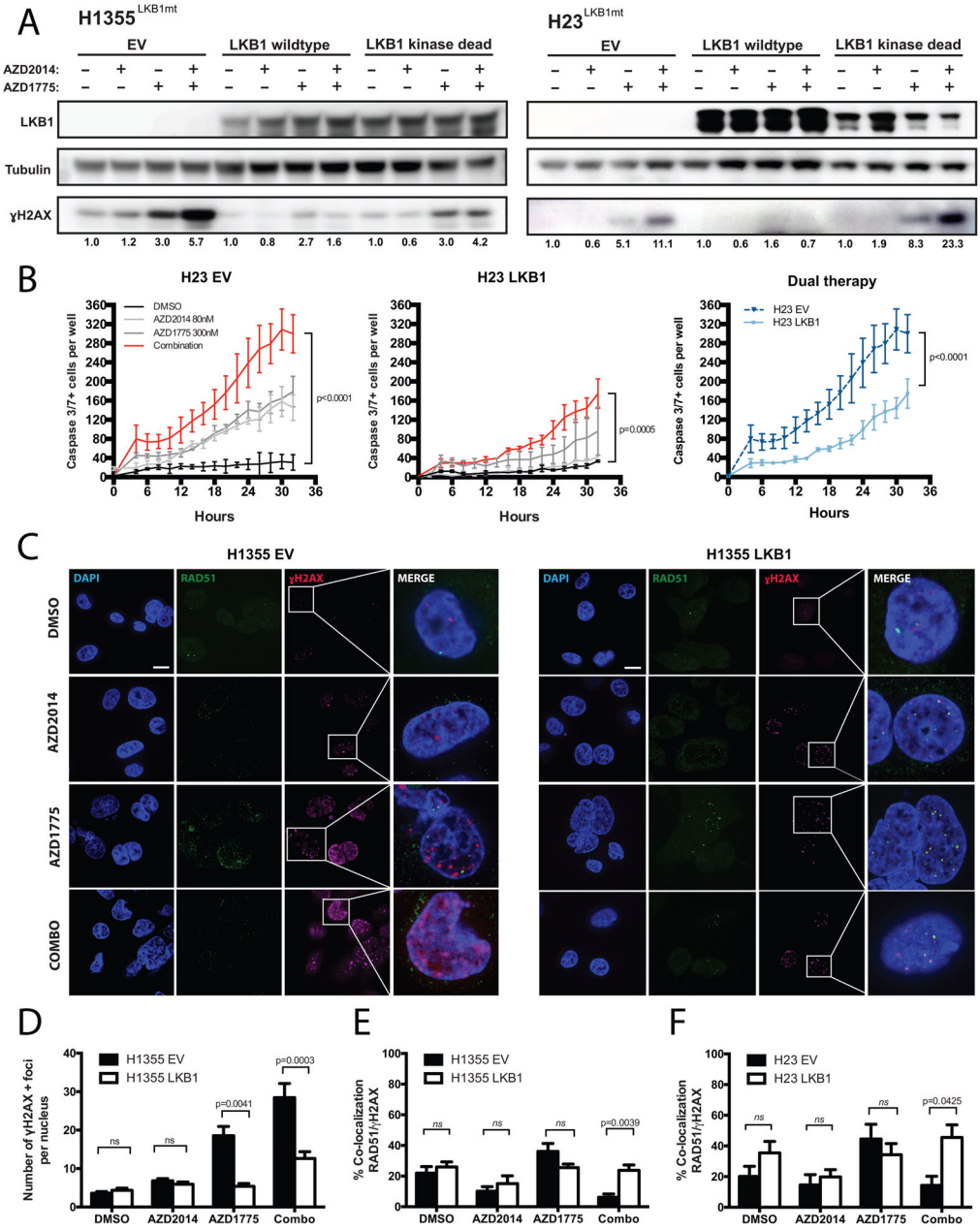

Figure 6. Loss of LKB1 in KRAS-mutant cell lines confers sensitivity to dual WEE1 and mTOR therapy due to impaired HR repair

(A) Western blot analyses on H1355 and H23 expressing either empty vector (EV) control, human wild type (WT) LKB1, or kinase-dead (KD) LKB1 showed changes in γH2AX protein levels after treatment with either AZD2014 (80nM), AZD1775 (300nM), or dual therapy for 48 hours. Corresponding γH2AX protein quantification normalized to tubulin loading controls are shown below. (B) Live time-course imaging was used to measure the mean number of caspase3/7-positive cells upon indicated drug treatment on H23 EV cells (left panel) and H23 LKB1 cells (middle panel). Right panel shows a comparison between H23 EV and -LKB1 cells co-treated with AZD1775 and AZD2014. Each time point

represents 3 wells in duplicates (*n=6*). (C) Detection of RAD51, γ-H2AX and DAPI by immunofluorescence in H1355 cells expressing EV or LKB1 WT, untreated or treated with either AZD2014 (80nM), AZD1775 (300nM), or in combination. Representative foci-containing cells are shown at high power magnification (100x). Scale bar: 10μm. (D) Mean number of γH2AX-foci per nuclei after 48 hours of treatment with either 80nM AZD2014, 300nM AZD1775 or in combined agents. Over 80 nuclei were analyzed in H1355-LKB1 cells over three experiments. (E-F) Mean number of nuclei containing ≥ one γH2AX and RAD51 co-localized foci by immunofluorescence in H1355 (E) and H23 (F) cells including either EV or LKB1-WT constructs. Cells were treated with either 80nM AZD2014, 300nM AZD1775 or in combination for 48-hours. (ns: not significant, $p>0.05$)